ELSEVIER

Journal of Computational and Applied Mathematics 109 (1999) 261–280

JOURNAL OF COMPUTATIONAL AND APPLIED MATHEMATICS

The ZEUS code for astrophysical magnetohydrodynamics: new extensions and applications

James M. Stone

Department of Astronomy, University of Maryland, College Park, MD 20742-2421, USA

Received 13 November 1998; received in revised form 28 May 1999

Abstract

A brief review of the numerical methods implemented in the widely used ZEUS code for astrophysical magnetohydrodynamics (MHD) is given. Extensions of the numerical methods to treat problems in nonideal MHD in a variety of regimes are discussed. In particular, methods for treating Ohmic dissipation, and methods for studying partially ionized plasmas in which the ion and neutral components are weakly coupled through a collisional drag term are considered. Recent application of the methods to the study of the dynamics of accretion disks is described. © 1999 Elsevier Science B.V. All rights reserved.

Keywords: Magnetohydrodynamics; Methods: numerical; Accretion: accretion disks

1. Introduction

The vast majority of the visible plasma in the Universe contains a magnetic field. In many circumstances (for example, in the solar corona, in pulsar magnetospheres, and in many regions of the interstellar medium), the energy density in this field is at least as large as the internal or kinetic energy density in the plasma, so that it is an important if not dominant component to the dynamics. Even if the field is weak (in the sense that its energy density is small compared, e.g., to the thermal energy density) tension forces produced by bending the field lines can significantly alter the dynamics. For example, it is now known that weak magnetic fields are of fundamental importance in generating MHD turbulence and driving mass accretion in astrophysical disks [1]. Even the problem of how magnetic fields are amplified and maintained by currents associated with bulk flows in the plasma (a process termed a "dynamo") is not fully understood, but is the subject of active investigation [34]. It is clear that numerical methods for MHD will play a fundamental role in studies of these problems.

The addition of a magnetic field changes both the physics of the plasma, and the mathematical properties of the equations which describe it, in fundamental ways. Physically, the MHD equations contain three wave families (the fast and slow magnetosonic waves, and the Alfvén waves) as

0377-0427/99/$ - see front matter
PII: S0377-0427(99)00204-6

opposed to only the single acoustic wave family present in pure hydrodynamics. These additional wave families make the dynamics of the plasma much richer. The magnetosonic waves are compressive, meaning both modes support shocks and rarefactions. On the other hand, Alfvén waves are noncompressive shear waves, a mode which is completely absent in ideal hydrodynamics. Mathematically, the additional modes make solving the characteristic problem (which forms the basis of many modern numerical schemes for fluid dynamics [24]) much more difficult in MHD in comparison to hydrodynamics for two reasons. Firstly, there are seven characteristic curves in MHD (u, $u \pm v_{\mathrm{f}}$, $u \pm v_{\mathrm{A}}$, and $u \pm v_{\mathrm{s}}$, where u is the flow speed, and $v_{\mathrm{f}}, v_{\mathrm{A}}$, and v_{s} are the fast, Alfvénic, and slow mode speeds respectively), making the solution quite complicated. Secondly, the equations of MHD are not strictly hyperbolic, meaning that the eigenvalues corresponding to each characteristic are not always linearly independent. In addition, Maxwell's equations contain a constraint that the field must be divergence-free: there are no magnetic monopoles. Not only must one design a scheme which can evolve each wave mode in MHD accurately, but in addition the scheme must ensure the numerically evolved fields satisfy the divergence-free constraint.

There are two possible approaches to designing numerical methods for compressible MHD. The simplest is to solve the equations written in non-conservative form using an operator-split solution procedure [6]. There are a variety of astrophysical hydrodynamic codes that implement this method in one form or another (e.g., [35,22,26]); one well known example is the ZEUS code [45]. ZEUS solves the gas dynamic equations on a staggered mesh using high-order upwind methods to solve the advection terms, and an artificial viscosity to capture shocks. Covariant differencing forms are used to allow computation on any orthogonal coordinate system [29]. Both two- and three-dimensional versions are available, and the code has been implemented on architectures ranging from desktop workstations to distributed memory parallel supercomputers. The code is widely used, well documented in the literature [45], [46], [44], extensively tested [42], and it is publically available through the Laboratory for Computational Astrophysics (`http://www.lca.ncsa.uiuc.edu`).

It has been nearly eight years since a comprehensive description of ZEUS first appeared in the literature. In that time, improvements have been made to the method, and new extensions to the algorithm which allow the study of additional physics have been developed. In this paper, a description of these improvements and extensions will be given. Because the basic algorithms implemented in ZEUS have already been presented in detail in the literature, only a brief outline of the basic methods will be given here.

Since the first description of the ZEUS code appeared, there has been enormous progress in the development of numerical methods for MHD based on solving the equations in conservative form. In particular, Godunov methods [18] which are based on either a linear approximation, or a fully nonlinear solution, to the MHD Riemann problem are now widely used [25]. In addition, the use of adaptive meshes has proven very succesful for some applications. While there is an enormous range of problems that can be studied with the methods implemented in ZEUS, it is also likely that these new methods will see increasing use.

2. The ZEUS astrophysics code

The ZEUS code implements algorithms for three classes of problems: pure hydrodynamics [45], ideal MHD [46], and radiation hydrodynamics [44]. It is impossible to discuss the MHD methods

without first describing some of the basic properties of the hydrodynamical algorithm, thus important ingredients of the latter are described in this section. Discussion of the radiation hydrodynamical methods are beyond the scope of the present paper.

2.1. The ZEUS algorithm for ideal MHD

Before describing extensions to the basic MHD algorithms in ZEUS, we begin with an outline of the major components in the method. This description closely follows those given in [45,46,20].

In nonconservative form, the equations of ideal MHD are

$$\frac{\partial \rho}{\partial t} + \boldsymbol{\nabla} \cdot \rho \boldsymbol{v} = 0, \tag{1}$$

$$\frac{\partial \boldsymbol{S}}{\partial t} + \boldsymbol{\nabla} \cdot \boldsymbol{S}\boldsymbol{v} = -\boldsymbol{\nabla} p + \frac{1}{4\pi}(\boldsymbol{\nabla} \times \boldsymbol{B}) \times \boldsymbol{B}, \tag{2}$$

$$\frac{\partial e}{\partial t} + \boldsymbol{\nabla} \cdot e\boldsymbol{v} = -\frac{p}{\rho}\boldsymbol{\nabla} \cdot \boldsymbol{v}, \tag{3}$$

$$\frac{\partial \boldsymbol{B}}{\partial t} = -\boldsymbol{\nabla} \times \boldsymbol{E}, \tag{4}$$

where ρ is the mass density, $\boldsymbol{v}$ the velocity, $\boldsymbol{S}$ the momentum density, e the specific internal energy density, $\boldsymbol{B}$ the magnetic field, and $\boldsymbol{E}$ the electric field. The pressure p is related to e through an equation of state. For the simplest case of an adiabatic gas of noninteracting particles, the equation of state takes a simple form

$$p = (\gamma - 1)\rho e, \tag{5}$$

where γ is the ratio of specific heats. Most astrophysical plasmas are dominated by either monoatomic particles so that $\gamma = \frac{5}{3}$, or by molecular hydrogen, a diatomic molecule so that $\gamma = \frac{7}{5}$. In plasmas in which internal energy can be lost from the system via radiation on timescales very much shorter than dynamical timescales, an isothermal equation of state (i.e., $p = C_s^2 \rho$ where C_s is the isothermal sound speed) may be more appropriate. In this case the energy equation (3) can be dropped from the system. Under the assumptions of ideal MHD, the plasma conductivity is taken to be infinite, so that the only contribution to the electric field is from bulk motions of the plasma

$$\boldsymbol{E} = -\boldsymbol{v} \times \boldsymbol{B}. \tag{6}$$

As written above, it is clear that the terms on the RHS of the first three of the equations of ideal MHD represent sources and/or sinks of mass, momentum, and energy, respectively, whereas the terms on the LHS represent transport of conserved quantities via advection. An operator split solution procedure divides the update of these two terms into two separate steps (see [6] for a description of the mathematical basis of the method). In the first step, hereafter called the *transport step*, the terms on the LHS of the equations are updated in conservative form using higher-order upwind methods. This step is described in detail in Section 2.3. In the second step, hereafter called the *source step*, simple finite differences are used to evaluate the terms on the RHS of the equations. Additional terms must be added in order to capture shocks. This step is described in Section 2.4 below. Note that

the induction Eq. (4) can not be represented in this splitting, moreover the mathematical constraints introduced by Maxwell's equations implies that an operator split method will not give accurate solutions. Thus, the induction equation must be updated with entirely different methods: these are described in Section 2.5.

2.2. The numerical grid

The most basic property of any grid-based numerical algorithm is the representation of the dependent variables on the numerical mesh. In a finite domain $(0:L_x;0:L_y;0:L_z)$ the continuous independent variable $\boldsymbol{x}$ is transformed into discrete values in each coordinate direction, i.e., $x \rightarrow x_i$ where $x_i = (i - 1/2)\Delta x$, $i = 1,\ldots,N_x$ is the location of cell centers, and $\Delta x = L_x/N_x$. Similarly, the y-, and z-coordinates are discretized into y_j and z_k using N_y and N_z zones with corresponding grid sizes Δy and Δz. The grid spacing in any direction need not be uniform, although for simplicity here it is taken to be so. Each dependent variable must then be represented as discrete values located either at the centers of cells, or at the faces of cells. Numerical schemes which use the nonconservative form generally use *staggered meshes*, meaning that scalar quantities such as the density and pressure are located at cell centers, while components of vectors are located on the corresponding cell face with a parallel surface normal vector (implying the different components of vectors are located on different cell faces). In either case, the continuous variable $a(\boldsymbol{x})$ is then represented as discrete values $a_{i,j,k}$ on this mesh, with whole (half) integer subscripts representing centering at cell centers (faces). It is important to emphasize that rather than being the pointwise values of the true solution (i.e., $a(x_i, y_j, z_k)$), these discrete values instead represent a cell average, so that $a_{i,j,k} \equiv (\int a(\boldsymbol{x})\,\mathrm{d}\boldsymbol{x})/\Delta x\Delta y\Delta z$, where the integration spans the volume of the zone centered on $a_{i,j,k}$. Boundary conditions must be supplied for each variable at every edge of the domain, usually by specifying the values $a_{0,j,k}$ and $a_{N+1,j,k}$ (and similarly for the y- and z-directions) in "ghost" or "guard" cells beyond the domain of the computational grid. Fig. 1 shows the positioning of the dependent variables in the numerical grid used by the ZEUS code.

We have implicitly adopted a Cartesian coordinate system in describing the spatial mesh described above. In fact, ZEUS uses a covariant differencing scheme in which all vector and tensor operators are represented using metric scale factors. This allows the difference equations to be general, so that the code in principle can compute in any orthogonal coordinate system. In practice, however, there are subtleties in each coordinate system which must be dealt with individually. For example, as described in [29,4], in a curvilinear mesh variables should be treated as being located at the volume center, rather than the geometric center, of zones. This modifies the spatial interpolation formulae, and some finite-difference formulae, used in the algorithm. In addition, coordinate singularities (across which the finite-difference representation of some opertors may diverge) in, e.g., spherical polar or cylindrical meshes, must be handled on a case-by-case basis. Thus, ZEUS is intended to be used in one of three coordinate systems: Cartesian, cylindrical, or spherical polar. A full description of the covariant differencing formalism is given in [45].

In addition to discretization in the spatial domain, a numerical solution to the PDEs must also be descretized in time. At the initial time values for all dependent variables are specified over the entire spatial grid. These values must be stepped forward using a timestep Δt chosen by the numerical algorithm. This results in a four-dimensional grid of data for each variable $a^n_{i,j,k}$, $n = 0,\ldots,M$, where the superscript denotes the time level. Note that in practice the timestep will not be constant

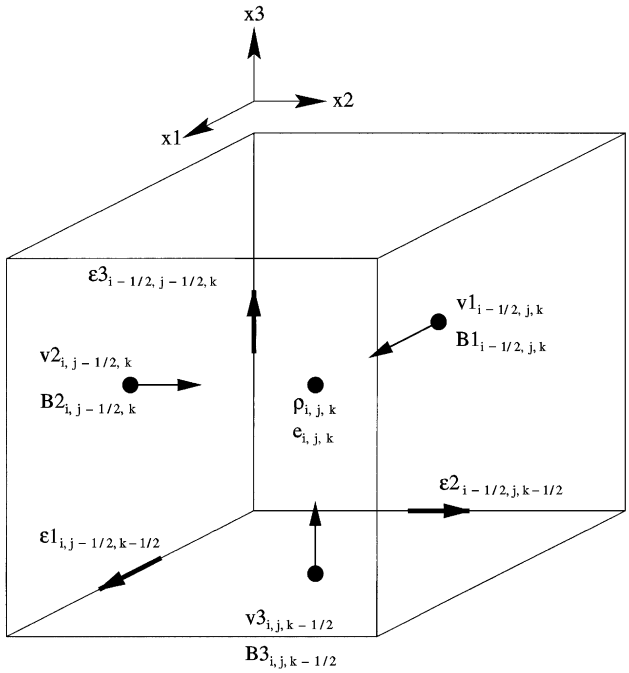

Fig. 1. Centering of variables in the ZEUS code. One zone of the computational mesh is shown. The density ρ and specific internal energy density e are located at cell center, the components of the velocity $\boldsymbol{v}$ and magnetic fields $\boldsymbol{B}$ are face-centered, while the electromotive forces used to update the magnetic field (see Section 2.5) are edge-centered.

over all the steps. Instead, for an explicit time-differencing method (in which case all terms are evaluated using known data at the current time level n) such as used by ZEUS, the timestep must be chosen to satisfy a stability constraint; for example the Courant–Friedrichs–Lewy [10] condition: $\Delta t \leqslant \Delta x/\max(\|\boldsymbol{W}_{i,j,k}\|)$, where the components of $\boldsymbol{W}$ are the characteristic speeds in the equations. Since the $\boldsymbol{W}_{i,j,k}$ depend on the solution, this condition must be applied at each timestep, so that in general Δt will not be constant. In an operator split method, one need not adopt the same time-differencing algorithm for all the terms. Thus, for stiff terms (those in which the characteristic time of variation is much shorter than the dynamical time in the flow) it may be useful to use a implicit method (in which case all terms are evaluated using suitable averages of data at the current and advanced time). In this case the finite-difference formula result in a set of coupled nonlinear equations which must be solved for the unknowns $a^{n+1}_{i,j,k}$. The only constraints placed on the timestep in an implicit method are those set by accuracy, and by the convergence properties of the nonlinear solver.

2.3. Advection algorithms — the transport step

The LHS of each of Eqs. (1)–(3) can be written as a set of scalar advection equations of the form

$$\frac{\partial a}{\partial t} + \frac{\partial (ua)}{\partial x} = 0, \tag{7}$$

where a represents the mass density, momentum density, and energy density respectively in each of Eqs. (1)–(3). Eq. (7) is manifestly in conservative form. An obvious, temporally second-order accurate finite-difference representation is

$$a_i^{n+1} - a_i^n = \frac{\Delta t}{\Delta x}(\boldsymbol{F}_{i+1/2}^{n+1/2} - \boldsymbol{F}_{i-1/2}^{n+1/2}), \tag{8}$$

where for simplicity the system has been restricted to one spatial dimension. (A multidimensional version of the method is constructed by performing sets of one-dimensional sweeps along orthogonal coordinates at each timestep, a process called directional splitting [47].) Here, $\boldsymbol{F}(a_{i+1/2}^{n+1/2})$ denotes the fluxes of a. Note the fluxes are located halfway between the values a_i, and that to achieve centered temporal differencing they must be evaluated using time averaged values of a. (Generally, it is sufficient to approximate the time average of the fluxes with the flux computed using the time averages of a.)

Much of the complexity in numerical schemes for gas dynamics is associated with finding an accurate and stable representation of the time averaged fluxes in Eq. (8). There are two very different kinds of error which must be minimized. The first is diffusion error associated with the spatial spreading of sharp features in the initial data as it is evolved. Generally, diffusive errors are reduced by adopting spatially higher-order schemes. The second type of error is dispersion error. This is associated with the propagation of different spatial frequencies in the initial data at different velocities. A wavepacket made up of many different frequencies will therefore disperse, or spread apart, as it propagates. Alternatively, pure modes may simply propagate at the wrong speed. Dispersive errors are generally only apparent in high-order schemes: low-order schemes are so diffusive any dispersive error is swamped. In fact, one common technique to reduce the appearance of dispersive errors is to add diffusion.

One of the most straightforward techniques for computing the fluxes in Eq. (8) is to use a predictor-corrector scheme such as the two-step Lax–Wendroff method (e.g., [32]). This gives second-order spatial accuracy for smooth regions, but unfortunately the scheme has a large dispersion error which requires the addition of large amounts of diffusion. Hybrid methods which use the Lax–Wendroff flux in smooth regions, but a low-order and less dispersive flux near discontinuities have proven successful: such methods are termed "flux-limiter" methods, an example is the flux-corrected transport (FCT) scheme [5,48]. Both the two-step Lax–Wendroff and the FCT method are widely used for applications in astrophysics.

One important technique that can be used to reduce dispersion error is to use a difference molecule that utilizes information which is upstream of the interface. If $u =$ constant, the solution to Eq. (7) is simply $a(x,t) = a(x - ut, t = 0)$, i.e., the original function displaced by an amount ut. Clearly, then, the appropriate fluxes $F(U_{i+1/2}^{n+1/2}) = a_{i+1/2}^{n+1/2}u$ in a finite-difference representation of Eq. (7) are simply the total amount of a passing through the interfaces in Δt. For a scalar advection equation it is straightforward to compute this quantity by integrating the amount of a upstream of the interface within the domain of dependence $u\Delta t$. As described below, high-order representations of this integral can be constructed by accounting for the spatial variation of a within grid cells using piecewise continuous interpolation formulae. Nonlinear stability of upwind schemes requires the interpolation scheme must be monotonicity preserving, that is the interpolation must not introduce any new extrema into the data. More generally, it can be shown that if an interpolation scheme reduces the total variation of the solution, that is the sum of the difference of the solution between neighboring

grid points, then the scheme will be nonlinearly stable. Such "total variation diminishing" (TVD) interpolation schemes can be proven to be monotonicity preserving, and moreover, they can be shown to guarantee convergence to the weak solution of the PDE [25,19]. TVD and monotone methods are an essential ingredient to upwind schemes because they eliminate oscillations (overshoots) introduced by interpolation near discontinuities in the solution.

The order of the interpolation formulae used to construct the fluxes determines the spatial order of upwind methods. Several techniques are commonly used:

1. *Donor cell* (*first order*) *method.* The simplest interpolation scheme is to assume that the variable a is constant within a zone, leading to the upwinded values

$$a_{i-1/2}^{n+1/2} = \begin{cases} a_{i-1}^n & \text{if } u > 0, \\ a_i^n & \text{if } u < 0. \end{cases} \tag{9}$$

By ignoring any variation of a within a zone, the donor cell method is quite diffusive and therefore is not acceptable in applications.

2. *van Leer* (*second order*) *method.* A second-order scheme can be constructed by using a piecewise linear function to represent the distribution of a within a zone (e.g., [53]),

$$a_{i-1/2}^{n+1/2} = \begin{cases} a_{i-1}^n + (\Delta x - u\Delta t)(\delta a_{i-1}^n/2) & \text{if } u > 0, \\ a_i^n - (\Delta x + u\Delta t)(\delta a_i^n/2) & \text{if } u < 0, \end{cases} \tag{10}$$

where the δa_i^n are the monotonized, van Leer slopes computed from the harmonic average

$$\delta a_i^n = \begin{cases} \dfrac{2(\Delta a_{i-1/2}\Delta a_{i+1/2})}{\Delta a_{i-1/2} + \Delta a_{i+1/2}} & \text{if } \Delta a_{i+1/2}\Delta a_{i-1/2} > 0, \\ 0 & \text{otherwise,} \end{cases} \tag{11}$$

and $\Delta a_{i+1/2} = (a_{i+1}^n - a_i^n)/\Delta x$. The definitions of the van Leer slopes in Eq. (8) can be extended to account for a nonuniform grid spacing. Note that when the van Leer slopes are zero, the method reduces to the donor cell (first order) method given in Eq. (5). Other forms of the slope limiters are possible [33,52]: it is the slope limiter that makes the scheme monotone and therefore preserves nonlinear stability. The second-order method offers the advantages of improved accuracy (less diffusion) combined with speed, and is therefore widely used in astrophysical applications.

3. *PPM* (*third order*) *method.* The piecewise parabolic method (PPM) for advection uses parabolic interpolation within a zone to compute upwinded interface values. The entire interpolation procedure, combined with the monotonicity constraints that ensure nonlinear stability, are too complex to reproduce here, they are given in [9]. By using parabolae for interpolation, the PPM method requires that two points be specified upwind of the interface. In general, the PPM method uses a five-point molecule centered on the zone being updated. Thus, at boundaries, values must be specified for two ghost zones beyond the computational domain.

Fig. 2 compares the solution to the scalar advection Eq. (7) computed using these three upwind schemes for a test problem consisting of the advection of a square pulse originally 100 zones wide a distance of 10 times its width. Note the first-order method results in unacceptable diffusion of the pulse. In fact, the scheme will continue to diffuse the pulse so that its amplitude continues to decrease as it propagates. The second- and third-order schemes show enormous improvement in the

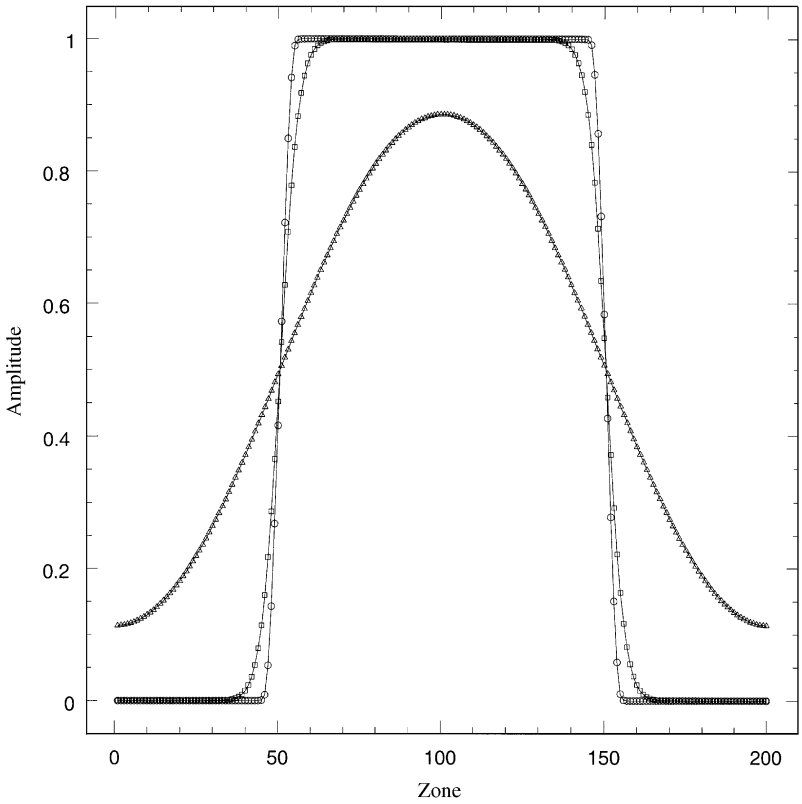

Fig. 2. Result from advecting a square pulse a distance of 10 times its width using first-order (triangles), second-order (squares), and third-order (circles) upwind methods.

solution: the pulse edges become about 30 and 10 zones wide, respectively. In fact, the third-order alogorithm can be improved by specially designed switches that detect discontinuities and modify the interpolation formulae accordingly, resulting in edges that are 2–3 zones wide [9]. Moreover, in the higher-order schemes the pulse shape becomes fixed with time rather than continuously decaying. As described above, the schemes assume the advection velocity u does not vary spatially. In order to preserve their formal convergence properties in the presence of a spatially varying velocity, they must be modified in a straightforward way [16].

2.4. Shock capturing with an artificial viscosity

The transport module described above, which updates the LHS of Eqs. (1)–(3), forms the first step in the operator split solution procedure implemented in ZEUS. The second step is to add the source terms on the RHS of these equations. As described in [45], straightforward finite-difference representations of these terms can be written for the staggered mesh used by ZEUS. These representations are written out in full in [45], and thus will not be repeated here.

However, simply adding the source terms to the advection step is not enough to complete the hydrodynamic algorithm. The obvious nonlinearities in the LHS of Eq. (2) (which, when the RHS is taken to be zero, should be recognized as Burgers' equation) are of great interest in their own right; they lead to the steepening of smooth solutions into discontinuities (shocks in the case of gas dynamics). Since the PDEs will break down in discontinuities, finite-difference formula will also fail there. A simple solution is to add dissipation near discontinuities to smooth them over many grid zones so that the finite difference operators can still be applied.

The customary approach for smoothing shocks is to introduce a scalar artificial viscous pressure which is a nonlinear function of the compression, and therefore gives the correct entropy jump across shocks and the correct shock propagation velocity, while having negligibly small effect elsewhere. The most common formulation for this viscous pressure is in [54].

$$q = \begin{cases} l^2\rho(\nabla \cdot \boldsymbol{v})^2 & \text{if } \nabla \cdot \boldsymbol{v} < 0, \\ 0 & \text{otherwise,} \end{cases} \tag{12}$$

where l is a constant with dimensions of length which determines the strength of the artificial viscosity. Typically, l is chosen to be a few times Δx. Alternative formulations for this viscous pressure in curvilinear coordinates are given in [51]. Incorporation of this artificial viscosity into the algorithm simply requires adding a viscous pressure term $-\nabla q$ to the RHS of the momentum Eq. (10), and a viscous heating term $-q(\nabla \cdot \boldsymbol{v})$ to the RHS of the energy Eq. (12). Note that to observe convergence of a shock profile computed with an artificial viscosity, it is necessary to hold l itself constant, rather than the ratio of $l/\Delta x$, since as with all numerical methods the shock profile is fixed relative to the zone number [23].

Artificial viscosity is not required to make the above algorithm stable, rather it is needed to thermalize kinetic energy in shocks. Without the viscosity, there are large-amplitude post-shock oscillations which are not easily damped and which contain the kinetic energy flux propagating through the shock front. However, these oscillations are bounded, and the scheme will run stably with them (examples of shock profiles computed with and without an artificial viscosity are given in Figs. 12.3 and 12.4 of [32]). It should also be realized that some numerical methods which use the conservative form (for example the two-step Lax–Wendroff scheme) also require the use of an artificial viscosity to capture shocks properly. Godunov schemes which use a nonlinear Riemann solver to compute the interaction of discontinuous states, and therefore the fluxes of conserved quantities through cell faces, do not require an artificial viscosity to capture shocks except in special circumstances [9] (for example, shocks which are nearly stationary with respect to the grid). Because the Riemann solver is constructed specifically to account for nonlinear wave interactions, Godunov schemes for hydrodynamics generally are more accurate for shock dynamics than schemes which use an artificial viscosity.

Fig. 3 demonstrates the differences in the profiles of shocks computed using a Godunov scheme (a PPM code) and a nonconservative scheme which uses an artificial viscosity (the ZEUS code). Shown is the difference in the density profile computed by each scheme compared to the analytic solution for the Sod shocktube problem [40], i.e., the plot shows the error in the density. As expected, in both schemes the error is dominated by the discontinuities: either the shock near zone 186, or the contact discontinuity near zone 145. The rarefaction fan also is a source of error, especially the foot and head. Overall, the Godunov scheme results in considerable thinner shocks, and an overall error which is lower by a factor of a few.

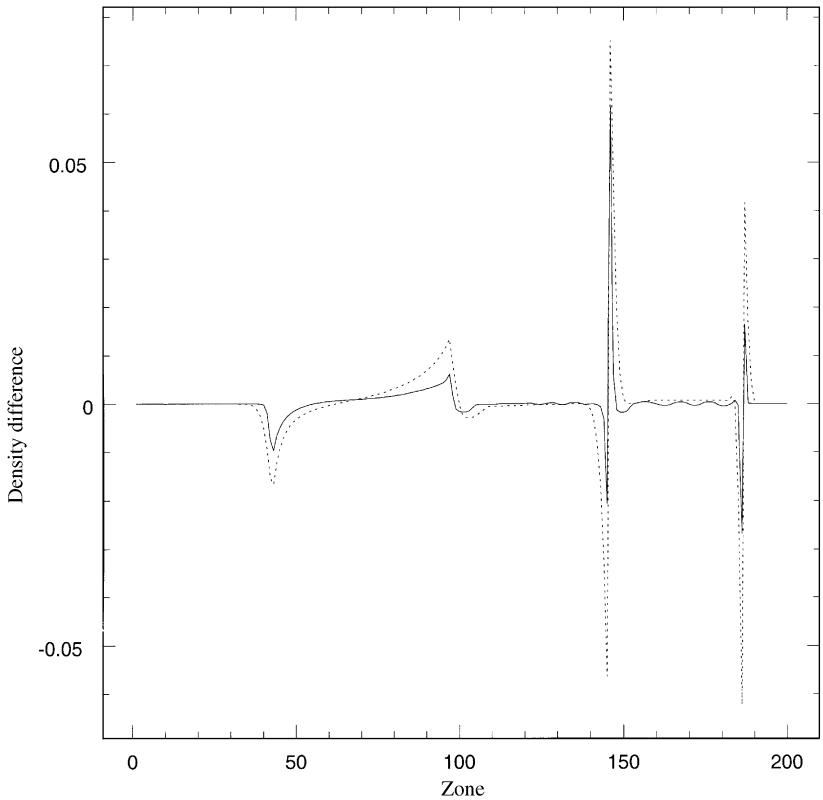

Fig. 3. Error in the density for the Sod shocktube problem for a solution computed using the ZEUS code (dashed line) and a PPM code (solid line).

2.5. Evolving the induction equation — the MOCCT algorithm

It is clear that the induction Eq. (4) can not be solved using an operator split solution procedure described above, since it can not be written as a transport equation for a conserved quantity. However, there is yet an additional complexity: one must ensure the evolved field satisfies the divergence-free constraint imposed by Maxwell's equations

$$\boldsymbol{\nabla} \cdot \boldsymbol{B} = 0. \tag{13}$$

In general, a numerical differencing scheme for the induction equation will not guarantee that the truncation error added as the field is evolved satisfies the divergence-free constraint. Thus, an initially divergence-free field will not remain so as it is evolved. An important question is: does the addition of divergence in the magnetic field at the level of the truncation error matter? The work in [7] was the first to demonstrate that it probably does: by comparing solutions to a test problem in which the forces proportional to $\boldsymbol{\nabla} \cdot \boldsymbol{B}$ were removed with solutions to this same problem in which these forces were not removed, these authors discovered widely disparate results. Other authors have compared the evolution of certain MHD problems in one or two dimensions using schemes that either did or did not enforce the divergence-free constraint, in many cases reporting no significant difference in the

results (e.g., [11,55]). The fundamental question is whether the truncation error in the divergence part of the field with these schemes is random and uncorrelated so that it does not grow with time. It seems quite possible that for a complex, three-dimensional flow in which the magnetic field becomes highly tangled and disordered (for example, in turbulent flows), accurate solutions will require a method which keeps the numerically evolved field consistent with the divergence-free constraint to a high degree of precision. Unfortunately, tests involving complex multidimensional field geometries simply have not been reported in the literature as of yet.

Because of the divergence-free constraint, the induction equation (4) must be treated with special techniques. One of the simplest ideas for a numerical scheme that enforces the divergence-free constraint is to represent the magnetic field using vector potentials $\boldsymbol{A}$, from which the field is derived through $\boldsymbol{B} = \boldsymbol{\nabla} \times \boldsymbol{A}$. Using the transverse gauge, the induction equation written in terms of the vector potential becomes a simple transport equation [6]. The advantage of this approach is that since $\boldsymbol{\nabla} \cdot (\boldsymbol{\nabla} \times \boldsymbol{A}) = 0$, a method based on evolving the vector potential guarantees the divergence-free constraint is satisfied. The disadvantage is that evaluating the Lorentz force requires taking a numerical second derivative. For smooth flows this method can work well, but in regions with sharp gradients in the potential (such as shocks or current sheets), the Lorentz force often contains overshoots which can only be fixed by smoothing. Still, a number of astrophysical application codes use the vector potential approach, these include some methods based on the conservative form (such as two-step Lax–Wendroff codes [38]), and some algorithms based on the nonconservative form (e.g., [31]).

Schemes which evolve the magnetic field directly will clearly be at an advantage in treating sharp boundaries in comparison to vector potential schemes. Evans and Hawley [14] realized it is possible to construct a multidimensional, conservative differencing scheme for the magnetic flux provided the appropriate control volume is used, and so ensure the divergence-free constraint is enforced. The method begins by using Stokes' theorem to write the induction equation as

$$\frac{\partial \Phi}{\partial t} = \oint_{\partial S} (\boldsymbol{v} \times \boldsymbol{B}) \cdot \mathrm{d}l, \tag{14}$$

where $\Phi = \boldsymbol{B} \cdot \mathrm{d}\boldsymbol{A}$ is the magnetic flux through a surface S of area $\mathrm{d}\boldsymbol{A}$ bounded by ∂S. The discretization scheme is then developed as follows. Each computational zone defines a cube in three-dimensional space (see Fig. 1). The components of the magnetic field are centered on the faces of this cube, with the x-component located on the cell face whose normal component is parallel to the x-direction, i.e., a staggered mesh is used. The components of the magnetic flux $\Phi_{i,j,k}$ are then simply the product of each component of the field with the area of the cell face on which it resides, for example $\Phi_{i-1/2,j,k} = B1_{i-1/2,j,k} \Delta y \Delta z$. The integrand in Eq. (14) is the electromotive force (EMF); in a finite difference representation the EMF must be located along cell edges (see Fig. 1), so that the integral represents the sum of the EMFs along the edges of the surface which contains Φ. Thus, in finite difference form, and using the centering of the components of $\boldsymbol{B}$ and the EMF (ε) described above (and shown in Fig. 1), the finite-difference form of Eq. (14) for the flux component colocated with $B1_{i-1/2,j,k}$ is

$$\begin{aligned}(\Phi^{n+1}_{i-1/2,j,k} - \Phi^{n}_{i-1/2,j,k})/\Delta t = {} & \varepsilon 2_{i-1/2,j,k-1/2} \Delta y + \varepsilon 3_{i-1/2,j+1/2,k} \Delta z \\ & - \varepsilon 2_{i-1/2,j,k+1/2} \Delta y - \varepsilon 3_{i-1/2,j-1/2,k} \Delta z.\end{aligned} \tag{15}$$

Note the sign of the terms in Eq. (15) are determined by whether the EMFs are parallel or antiparallel to the coordinate directions. Similar equations can be written for the update of the flux on the other five faces of the computational zone shown in Fig. 1.

The divergence-free constraint (Eq. (13)) then requires that the sum of the differences of the fluxes between opposing faces be zero, i.e.,

$$\frac{\Phi_{i+1/2,j,k} - \Phi_{i-1/2,j,k}}{\Delta x} + \frac{\Phi_{i,j+1/2,k} - \Phi_{i,j-1/2,k}}{\Delta y} + \frac{\Phi_{i,j,k+1/2} - \Phi_{i,j,k-1/2}}{\Delta z} = 0. \tag{16}$$

Since all six faces of the cube share the same edges, the update of the magnetic flux on each surface uses the same EMFs. This lies at the heart of the scheme. If one computes the finite-difference representation of the divergence at the advanced time (Eq. (16)) by algebraically inserting the time-advanced fluxes computed from Eq. (15) (and the update equations for the other five components of the flux), each EMF will appear twice on the RHS, once each with opposite sign, and therefore all the EMFs cancel. The net result is that time-advanced magnetic flux also obeys the divergence-free constraint (14) analytically. Because the update of the magnetic fluxes has used the same EMFs, the scheme is conservative. It is analogous to a conservative differencing formula for the gas dynamic equations that uses the same flux between neighboring cells and therefore conserves mass, momentum, and energy exactly. The technique was called constrained transport (CT) in [14].

Note an essential point is that the solution of the induction equation is not directionally split, that is all three components of the magnetic field must be updated at once using the same EMFs. This will be a fundamental property of any method that preserves the divergence-free constraint.

To this point, no mention has been made of how the EMFs should actually be computed. In fact, it does not matter what EMFs are used in Eq. (15), the CT scheme will preserve the divergence-free constraint. Of course, in practice, a method must be used which gives accurate representations of the time-averaged EMFs. Through a series of test problems for MHD, Stone and Norman [46] found that solving the characteristic equation for Alfvén waves to compute time-averaged EMFs in the CT scheme gave the best results. A critical step in the method is to difference the Lorentz force term in Eq. (2) using the time-averaged magnetic fields which result from the solution of the Alfvén wave characteristic equations in the CT scheme. The full scheme is referred to as MOC-CT; a complete description is given in [46], test problems used to calibrate the method are described in [42], and recent advances and updates to the method are given in [20]. Given that the finite-difference equations used to construct a multidimensional version of the algorithm are given in detail in these references, they will not be repeated here. An alternative formulation of an improved MOC-CT algorithm to that described in [20] is given in [8].

3. Extension of ZEUS to nonideal MHD

The MHD algorithm implemented in ZEUS and discussed above is designed for ideal plasmas, i.e., those which have infinite conductivity. In many astrophysical systems, the temperature of the plasma is so low that the ionization fraction f (the ratio of the electron number density n_e to neutral particle number density — which can be taken to be the number density of hydrogen atoms n_H since in astrophysical plasmas neutral hydrogen dominates all other elements) is extremely small. If f becomes so small that the ions (and therefore the magnetic field, which is coupled directly only to

the ions) begin drifting with respect to the neutrals, then the magnetic field is no longer coupled to the bulk of the fluid (the neutrals), and the assumptions of ideal MHD breakdown. There are several regimes of interest in this case, each of which can be described by different approximations in the equations of motion. If the number density of the plasma is very large, so that the ion–neutral collision rate is also large compared to the ion gyrofrequency, then the effect is to damp electrical currents in the plasma through an Ohmic resistivity. This can be treated by the addition of a finite conductivity term to Ohm's law (Eq. (6)). On the other hand, if the ion–neutral collisions are infrequent compared to the ion gyrofrequency, then the ion and neutrals begin to behave as two independent fluids coupled through a collisional drag term. In this case the dynamics of the plasma must be described by separate systems of conservation laws for the ions and neutrals. Finally, if the ion and neutral densities are not independent but assumed to be in ionization equilibrium, then one can simplify the coupled ion and neutral equations of motion to a single fluid system with a nonlinear diffusion term in the induction equation. Numerical methods to treat each of these regimes have recently been implemented in the ZEUS code as described below.

3.1. Incorporating ohmic resistivity

In a resistive plasma, Ohm's law can be written

$$\boldsymbol{E} = -\boldsymbol{v} \times \boldsymbol{B} + \eta \boldsymbol{J}, \tag{17}$$

where η is the resistivity of the plasma (inverse of the conductivity). In writing Eq. (17) several approximations have been made; the contribution to the current from the Hall term present in a generalized formulation of Ohm's law has been dropped, and the conductivity tensor has been assumed to be isotropic.

With the addition of a finite resistivity, the induction equation can be written in integral form as

$$\frac{\partial \boldsymbol{\Phi}}{\partial t} = \oint_{\partial S} (\boldsymbol{v} \times \boldsymbol{B}) \cdot \mathrm{d}l - \eta \oint_{\partial S} \boldsymbol{J} \cdot \mathrm{d}l. \tag{18}$$

In designing a numerical method to solve this equation, it is important that the solution procedure enforces the divergence-free constraint. The CT method for updating the first term on the RHS of Eq. (18) was described above. Clearly, the second term on the RHS can be differenced using the CT formalism described in Section 2.5, with the effective EMF for the resistive term simply equal to the current density $\boldsymbol{J}$ in this case. Using the staggered mesh shown in Fig. 1, it is straightforward to write down finite-difference representations for $\boldsymbol{J}$, for example

$$J1_{i,j-1/2,k-1/2} = \frac{(B3_{i,j,k-1/2} - B3_{i,j-1,k-1/2})}{\Delta y} - \frac{(B2_{i,j-1/2,k} - B2_{i,j-1/2,k-1})}{\Delta z}. \tag{19}$$

Note that for a staggered mesh, the components of the current are automatically centered at the appropriate locations to be used as EMFs in the update of the magnetic flux using the CT scheme.

A numerical scheme based on the CT approach to differencing the resistive term has been developed in [17]. The resistive term is operator split from the rest of the induction equation, that is MOC-CT is first used to update the fields using the first term in Eq. (19), and the resistivity is added afterwards. One final important step is that for a time-explicit differencing formula for

the resistive term (which makes the induction equation a parabolic PDE) the timestep must satisfy a stability criterion of the form $\Delta t \leqslant (\Delta x)^2/\eta$. Because of the strong dependence of this limit on the grid spacing, it is very restrictive for high-resolution simulations, and in fact can completely dominate all other stability limits in the algorithm.

3.2. Treating partially ionized plasmas as a two-fluid system

If the ion-neutral plasma is only weakly coupled, the two species must be treated as separate fluids which obey distinct sets of conservation laws [13]. Using subscripts i and n to denote ion and neutral variables, respectively, the two sets of conservation laws take the following form:

$$\frac{\partial \rho_i}{\partial t} + \boldsymbol{\nabla} \cdot \rho_i \boldsymbol{v}_i = 0, \tag{20}$$

$$\frac{\partial \rho_n}{\partial t} + \boldsymbol{\nabla} \cdot \rho_n \boldsymbol{v}_n = 0, \tag{21}$$

$$\frac{\partial \boldsymbol{S}_i}{\partial t} + \boldsymbol{\nabla} \cdot \boldsymbol{S}_i \boldsymbol{v}_i = -\boldsymbol{\nabla} p_i + \frac{1}{4\pi}(\boldsymbol{\nabla} \times \boldsymbol{B}) \times \boldsymbol{B} + \alpha \rho_i \rho_n (\boldsymbol{v}_n - \boldsymbol{v}_i), \tag{22}$$

$$\frac{\partial \boldsymbol{S}_n}{\partial t} + \boldsymbol{\nabla} \cdot \boldsymbol{S}_n \boldsymbol{v}_n = -\boldsymbol{\nabla} p_n - \alpha \rho_i \rho_n (\boldsymbol{v}_n - \boldsymbol{v}_i), \tag{23}$$

$$\frac{\partial \boldsymbol{B}}{\partial t} = \boldsymbol{\nabla} \times (\boldsymbol{v}_i \times \boldsymbol{B}). \tag{24}$$

An isothermal equation of state has been adopted for both species, so that the energy equation can be dropped from the system. The ion and neutral pressures are thus given by $p_i/\rho_i = p_n/\rho_n = C_s^2$, where C_s is the isothermal sound speed. Extending the system to nonisothermal fluids is straightforward.

The final terms in Eqs. (22) and (23) represent the collisional drag between the ion and neutral fluids [13]. The collisional coupling constant α is assumed to be independent of velocity. Note this term appears in each equation with opposite sign.

Ignoring for the moment the drag term, Eqs. (21) and (23) obviously form the equations of hydrodynamics for the neutrals, while Eqs. (20), (22) and (24) are the equations of ideal MHD for the ions. Thus, the hydrodynamical methods described above and in [45] can be used to solve Eqs. (21) and (23), while the MHD algorithms described above and in [46] can be used to solve Eqs. (20), (22) and (24). Because the drag term potentially is very stiff, it is best to use an implicit differencing formula for the update of this term. Since the drag term is linear in the velocity and does not involve any spatial operators, the implicit update formulae for these terms is particularly simple. Thus, to update the operator split drag term for the ion velocity

$$\frac{\partial \boldsymbol{S}_i}{\partial t} = \alpha \rho_i \rho_n (\boldsymbol{v}_n - \boldsymbol{v}_i) \tag{25}$$

the appropriate implicit finite-difference equation is

$$v_i^{n+1} = \frac{v_i^n + \alpha \Delta t (\rho_i v_i^n + \rho_n v_n^n)}{1 + \alpha \Delta t (\rho_i + \rho_n)}. \tag{26}$$

Similarly, the implicit difference formula for the operator split drag term in the neutral momentum equation results in

$$v_n^{n+1} = \frac{v_n^n + \alpha \Delta t(\rho_i v_i^n + \rho_n v_n^n)}{1 + \alpha \Delta t(\rho_i + \rho_n)}. \tag{27}$$

Note that in the limit of a very large timestep, these formula recover the correct asymptotic solution, namely the final velocities converge to the density-weighted averages of the initial values.

There are a variety of problems in the dynamics of the interstellar medium that can be investigated with a two-fluid algorithm for partially ionized plasmas as described above. Recently, this method has been used in [41,30] to study the Wardle instability in C-type MHD shocks. A closely related method has been used in [27] to study the same problem. It has also been used in [21] to study the nonlinear evolution of the magnetorotational instability in weakly ionized accretion disks. One primary difficulty with the method is that in some regions the ion density can become extremely small, leading to a divergence of the Alfvén speed, which therefore severly restricts the timestep that can be used in the explicit update of the ion-conservation laws. The solution of this problem is to adopt implicit differencing techniques [49].

3.3. Incorporating ambipolar diffusion

If both the ion inertia and the ion pressure are neglected in the two-fluid system of conservation laws equations (20)–(24), and the ion density is assumed to be in ionization equilibrium with the neutral density, so that $\rho_i = C\rho_n^{1/2}$ where C is a constant, then Eq. (22) can be solved for the ion velocity and inserted algebraically into Eqs. (23) and (24), thus reducing the system to the single fluid system equations (21), (23) and (24). In this case, however, the induction equation becomes complex [39]

$$\frac{\partial \boldsymbol{B}}{\partial t} + \boldsymbol{\nabla} \times (\boldsymbol{B} \times \boldsymbol{u_n}) = \boldsymbol{\nabla} \times \left\{ \frac{\boldsymbol{B}}{4\pi\alpha\rho_i\rho_n} \times [\boldsymbol{B} \times (\boldsymbol{\nabla} \times \boldsymbol{B})] \right\}. \tag{28}$$

Eq. (28) is a nonlinear diffusion equation for the magnetic field. Explicit differencing forms which ensure the divergence-free constraint is satisfied can be developed as outlined above. However, these forms encounter a restrictive stability constraint that make high-resolution simulations very expensive. The cost of explicit calculations can be reduced somewhat by subcycling, that is updating the induction equation many times in succession (with a timestep set by the stability constraint for the diffusion term) for each update of the full system of dynamical equations (at a timestep given by the usual CFL constraint). Fully implicit differencing forms for Eq. (28) are complex. An implementation of a numerical difference formula for the solution of Eq. (28) in the ZEUS code is given in detail in [28].

4. An example application

The methods implemented in the ZEUS code have proven to be useful tools for the study of MHD flows. Over the last ten years, they have been used to study an enormous variety of problems, indeed too large a variety to describe fully here. However, one useful example that demonstrates how such methods can be used to provide new physical understanding of astrophysical systems is

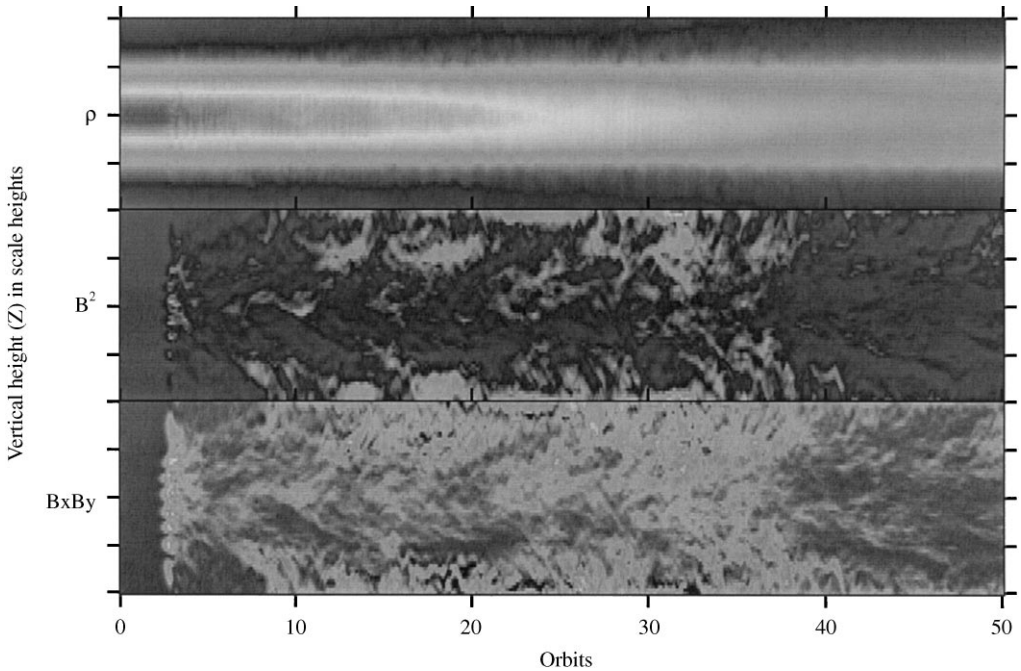

Fig. 4. Time evolution of the horizontally averaged density (top), magnetic energy (middle), and Maxwell stress (bottom) from a three-dimensional simulation of the nonlinear stage of the Balbus–Hawley instability in a weakly magnetized astrophysical accretion disk. MHD turbulence results after saturation of the instability at about 3 orbits.

provided by recent numerical studies of the nonlinear stage of a powerful, local, linear instability present in weakly magnetized accretion disks that regulates angular momentum transport [1]. Such disks are formed whenever plasma falls into a gravitational potential well. It has been a long-standing problem to uncover the source of angular momentum transport that allows accretion in disks, lately attention has focused on the MHD turbulence that is driven by the instability [1]. A variety of groups have applied techniques similar to the ZEUS MHD code to this problem (see [43] and references therein). Fig. 4 shows the time evolution of the horizontally averaged density, magnetic energy, and $B_x B_y$ component of the Maxwell stress tensor from a three-dimensional simulation of the evolution of this instability in a vertically stratified disk. After saturation of the instability at around 3 orbits of the disk, the flow is seen to be dominated by complex, turbulent motions with large values for the volume-averaged magnetic energy and stress. The most important physical result from the simulations is the finding that the turbulence results in vigorous angular momentum transport; many other findings are reported in [1,43] and the references therein.

In the dense regions of cold accretion disks around newly forming stars, the magnetic field may be only weakly coupled to the plasma. The evolution of the magnetorotational instability in resistive disks has also been studied numerically using the methods outlined in this paper. For resistive plasmas, Fleming et al. [17] found that MHD turbulence driven by the instability (and therefore angular momentum transport as well) is damped below magnetic Reynolds numbers of roughly 10^4. On the other hand, in weakly coupled ion–neutral disks, Hawley and Stone [21] found that the

instability saturates as complex structures in which the ions are squeezed into narrow sheets. Significant angular momentum transport occurs only if the neutral–ion collision frequency is of order 10^2 times the orbital period. Both of these studies extend our understanding of the nonlinear stage of the instability into more complex astrophysical systems.

5. Future development

In this article, some recent extensions of the ZEUS MHD code to the dynamics of nonideal plasmas have been discussed. In particular, methods for treating Ohmic resistivity, and for studying weakly coupled and partially ionized plasmas have been discussed. The importance of developing difference formulae in the paradigm of constrained transport in order to preserve the divergence-free constraint has been emphasized.

The methods described here are useful for the study of a wide range of problems in astrophysics. Current applications of the methods include problems in accretion disk dynamics, and in the formation and propagation of jets, among others. Moreover, the coupling of the methods to algorithms for radiation hydrodynamics as described in [44] has enabled applications in radiation MHD; for example, to the study of the dynamics of radiation-dominated accretion disks.

Recently, however, a variety of higher-order upwind methods for MHD based on the use of both linear and nonlinear Riemann solvers have been developed and have begun to see wide application in astrophysics [11,55,36,37,2,15]. Such methods have a distinct advantage over schemes based on the use of an artificial viscosity in their ability to treat shock dynamics; and therefore should be superior for MHD problems involving strong shocks and shock interactions. Preserving the divergence-free constraint in these methods is an important issue, and in fact most authors now adopt the constrained transport formalism described here for the integration of the induction equation.

The difficulty in developing Riemann solvers for more complex physical problems can be understood as the consequence of the introduction of new wave families (and characteristics) into the system. This also introduces the possibility of highly disparate time scales associated with wave families of greatly differing characteristic speeds. Often, the dynamics associated with the fastest time scale is not of interest; instead one wishes to evolve the flow on longer time scales associated with some other characteristic speed. An example includes MHD problems in weakly ionized media (where the Alfvén speed in the ions greatly exceeds the compressive waves speed in the neutrals). In such circumstances, methods which are implicit in the fastest characteristic speed, but not necessarily in the others, are of great utility. On the other hand, such methods are generally much more complex than fully explicit methods. Some implicit and semi-implicit versions of methods for MHD are presented in [12,50], further development and application of such methods to problems in astrophysics is very likely in the near future.

In addition to multiple time scales, many problems in astrophysics involve multiple length scales. For example, studying the dynamics of star formation requires resolving the newly formed protostellar core as well as the accretion flow which feeds it which may extend many orders of magnitude in spatial scale beyond the core. It is completely unpractical to resolve such flows with a fixed uniform grid. Nonuniform grid spacing is very useful for problems with a high degree of symmetry (for example spherically symmetric infall). Recently, adaptive and nested mesh methods have emerged as a promising method of resolving small subdomains within a larger volume (e.g. [3]). These methods

evolve the flow on subgrids using boundary conditions supplied by the coarser mesh solution. There is no limit to the number of levels of subgrids, implying an extremely large range of spatial scales can be achieved with the method. Such methods have been successfully applied using the PPM algorithm to problems in cosmology, accretion onto compact objects, the evolution of supernova explosions, as well as many others. It seems clear these methods will form the basis of many powerful astrophysical application codes in the future.

Acknowledgements

I thank my colleagues and collaborators S. Balbus, D. Clarke, C. Evans, J. Hawley, M. Norman, and D. Mihalas for their many contributions. I also wish to thank the National Science Foundation, NASA, and the DOE for financial support.

References

[1] S.A. Balbus, J.F. Hawley, Instability, turbulence, and enhanced transport in accretion disks, Rev. Mod. Phys. 70 (1998) 1–54.
[2] D.S. Balsara, TVD scheme for adiabatic and isothermal MHD, Astrophys. J. 116 (1998) 133–153.
[3] M. Berger, P. Colella, Local adaptive mesh refinement for shock hydrodynamics, J. Comput. Phys. 82 (1989) 64–84.
[4] J. Blondin, E. Lufkin, The PPM in curvilinear coordinates, Astrophys. J. (Suppl.) 88 (1993) 589.
[5] J.P. Boris, D.L. Book, Flux corrected transport I, SHASTA, a fluid transport algorithm that works, J. Comput. Phys. 11 (1973) 38–69.
[6] R.L. Bowers, J.R. Wilson, Numerical Modeling in Applied Physics and Astrophysics, Jones and Bartlett, Boston, 1991.
[7] J.U. Brackbill, D.C. Barnes, J. Comput. Phys. 35 (1980) 426.
[8] D.A. Clarke, A consistent method of characteristics for multidimensional magnetohydrodynamics, Astrophys. J. 457 (1996) 291.
[9] P. Colella, P.R. Woodward, The piecewise parabolic method for gas-dynamical simulations, J. Comput. Phys. 54 (1984) 174–201.
[10] R. Courant, K.O. Friedrichs, H. Lewy, On the partial difference equations of mathematical physics, IBM J. 11 (1967) 215–234.
[11] W. Dai, P.R. Woodward, Extension of the PPM to multidimensional ideal MHD, J. Comput. Phys. 115 (1994) 485–514.
[12] W. Dai, P.R. Woodward, A higher-order iterative implicit-explicit hybrid scheme for MHD, J. Comput. Phys. 124 (1996) 217.
[13] B. Draine, Interstellar shock waves with magnetic precursors, Astrophys. J. 241 (1980) 1021.
[14] C.R. Evans, J.F. Hawley, Astrophys. J. 332 (1988) 659.
[15] S.A.E.G. Falle, S.S. Komissarov, P. Joarder, A multidimensional upwind scheme for magnetohydrodynamics, Mon. Not. R. Astron. Soc. 297 (1998) 265.
[16] S. Finn, J.F. Hawley, Finite differencing the nonlinear continuity equation: velocity corrected transport, unpublished report, 1989.
[17] T. Fleming, J.M. Stone, J.F. Hawley, The effect of resistivity on the saturation of the magnetorotational instability Astrophys. J., submitted.
[18] S.K. Godunov, A finite difference method for the numerical computation and discontinuous solutions of the equations of fluid dynamics, Math. Sb. 47 (1959) 271.
[19] A. Harten, High resolution schemes for hyperbolic conservation laws, J. Comput. Phys. 49 (1983) 357–393.
[20] J.F. Hawley, J.M. Stone, MOCCT: A numerical technique for astrophysical MHD, Comput. Phys. Commun. 89 (1995) 127–148.

[21] J.F. Hawley, J.M. Stone, Nonlinear evolution of the magnetorotational instability in ion-neutral disks, Astrophys. J. 501 (1998) 758.
[22] J.F. Hawley, L.L. Smarr, J.R. Wilson, A numerical study of black hole accretion. II. Finite differencing and code calibration, Astrophys. J. (Suppl.) 55 (1984) 211–246.
[23] P.A. Kimoto, D.F. Chernoff, Convergence properties of finite difference hydrodynamic schemes in the presence of shocks, Astrophys. J. 96 (1995) 627–641.
[24] R.J. LeVeque, Numerical Methods for Conservation Laws, 2nd Edition, Lectures in Mathematics ETH Zurich, Birkhauser Verlag, Basel, 1992.
[25] R.J. LeVeque, in: O. Steiner, and A. Gautschy (Eds.), Nonlinear Conservation Laws and Finite Volume Methods, Computational Methods for Astrophysical Fluid Flow, Springer, Berlin, 1998.
[26] E.A. Lufkin, J.F. Hawley, The piecewise-linear predictor corrector code: A Lagrangian-remap method for astrophysical flows, Astrophys. J. (Suppl.) 88 (1993) 569–588.
[27] M.-M. MacLow, M. Smith, Nonlinear development and observational consequences of Wardle C-shock instabilities, Astrophys. J. 491 (1997) 596.
[28] M.-M. MacLow, M.L. Norman, A. Königl, M. Wardle, Incorporation of ambipolar diffusion into the Zeus magetohydrodynamics code, Astrophys. J. 442 (1995) 726.
[29] R. Mönchmeyer, E. Müller, A conservative second-order difference scheme for curvilinear coordinates I. Assignment of variables on a staggered grid, Astron. and Astrophys. 217 (1989) 351–367.
[30] D. Neufeld, J.M. Stone, The Wardle instability in interstellar shocks. II. Gas temperature and line emission, Astrophys. J. 487 (1997) 283.
[31] A. Nordlund et al, Astrophys. J. 392 (1992) 647.
[32] R.D. Richtmyer, K.W. Morton, Difference Methods for Initial Value Problems, 2nd edn., Interscience Publishers, New York, 1967.
[33] P.L. Roe, Some contributions to the modeling of discontinuous flows, Lecture Notes in Physics, vol. 141, Springer, Berlin, 1981.
[34] R. Rosner, Magnetic fields of stars, in magnetic activity in stars, galaxies, and quasars, Proc. Roy. Soc., in press.
[35] M. Rozyczka, Astron. Astrophys. 143 (1985) 59.
[36] D. Ryu, T.W. Jones, Numerical MHD in astrophysics: algorithm and tests for one-dimensional flow, Astrophys. J. 442 (1995) 228–258.
[37] D. Ryu, T.W. Jones, A. Frank, Numerical MHD in astrophysics: algorithm and tests for multidimensional flow, Astrophys. J. 452 (1995) 785–796.
[38] K. Shibata, Y. Uchida, Publ. Astron. Soc. Japan 37 (1985) 31–46.
[39] F. Shu, The Physics of Astrophysics. II. Gas Dynamics, University Science Book, Mill Valley, 1992.
[40] G.A. Sod, A survey of several finite difference methods for systems of nonlinear hyperbolic conservation laws, J. Comput. Phys. 27 (1978) 1–31.
[41] J.M. Stone, The Wardle instability in interstellar shocks. I. Nonlinear dynamical evolution, Astrophys. J. 487 (1997) 271.
[42] J.M. Stone, J.F. Hawley, C.R. Evans, M. Norman, A testsuite for astrophysical MHD simulations, Astrophys. J. 388 (1992) 415.
[43] J.M. Stone, J.F. Hawley, C.F. Gammie, S.A. Balbus, Three dimensional magnetohydrodynamical simulations of vertically stratified accretion disks, Astrophys. J. 463 (1996) 656.
[44] J.M. Stone, D. Mihalas, M.L. Norman, ZEUS-2D: a radiation magnetohydrodynamics code for astrophysical flows in two space dimensions: III. The radiation hydrodynamic algorithms and tests, Astrophys. J. (Suppl.) 80 (1992) 790–819.
[45] J.M. Stone, M.L. Norman, ZEUS-2D: A radiation magnetohydrodynamics code for astrophysical flows in two space dimensions: I. The hydrodynamic algorithms and tests, Astrophys. J. (Suppl.) 80 (1992) 753–790.
[46] J.M. Stone, M.L. Norman, ZEUS-2D: A radiation magnetohydrodynamics code for astrophysical flows in two space dimensions: II. The magnetohydrodynamic algorithms and tests, Astrophys. J. (Suppl.) 80 (1992) 791–818.
[47] G. Strang, On the construction and comparison of difference schemes, SIAM J. Numer. Anal. 5 (1968) 506.
[48] P.K. Sweby, High resolution schemes using flux limiters for hyperbolic conservation laws, SIAM J. Numer. Anal. 21 (1984) 995–1011.
[49] G. Tóth, Mon. Not. R. Astron. Soc. 274 (1995) 1002.

[50] G. Toth, R. Keppens, M.A. Botchev, Implicit and semi-implicit schemes in the VAC: numerical tests, Astron. Astrophys. 332 (1998) 1159–1170.
[51] W.-M. Tscharnuter, K.-H. Winkler, Comput. Phys. Commun. 18 (1979) 171.
[52] B. van Leer, Towards the ultimate conservative differencing scheme II. Monotonicity and conservation combined in a second-order scheme, J. Comput. Phys. 14 (1974) 361–370.
[53] B. van Leer, Towards the ultimate conservative differencing scheme IV. A new approach to numerical convection, J. Comput. Phys. 23 (1977) 276–299.
[54] J. Von Neumann, R.D. Richtmyer, A method for the numerical calculation of hydrodynamic shocks, J. Appl. Phys. 21 (1950) 232–237.
[55] A.L. Zachary, A. Malagoli, P. Colella, A higher-order godunov method for multidimensional ideal MHD, SIAM J. Sci. Comput. 15 (1994) 263–284.